Fast Measurement Methodology For Near Field Satellite Testing

F. D'Agostino[1], F. Ferrara[1], C. Gennarelli[1], R. Guerriero[1], M. A.Saporetti[2], F. Saccardi[2], L. J. Foged[2], D. Trenta[3]

[1] D.I.In. - Università di Salerno, via Giovanni Paolo II, 132, - 84084 Fisciano (SA), Italy, (fdagostino, flferrara, cgennarelli, rguerriero)@unisa.it

[2] Microwave Vision Italy SRL, Via dei Castelli Romani,59, Pomezia (RM), Italy, (maria.saporetti, francesco.saccardi, lars.foged)@ mvg-world.com

[3] European Space Agency, ESTEC, The Netherlands, Damiano.Trenta@esa.int

***Abstract*— In this paper, we present a fast measurement methodology applicable to near field testing of satellite in planar and spherical geometry using non-canonical scanning and irregular sampling. The planar measurements have been accomplished by the planar wide-mesh scanning (PWMS) approach [1], while the spherical measurements have been performed at the points of a nonredundant raster grid. In this grid, the number of the sampling parallels, as well as of the sampling point on them are drastically reduced. Both the nonredundant sampling representations are based on the two-bowls modelling of the antenna under test. Different test cases from satellite telecommunication are presented. These including a highly-shaped reflector antenna and a pencil beam antenna at Ku-band [2] and a Galileo navigation antenna, GIOVE B [3].**

The Near-Field to Far-Field transformation accuracy of the fast methodology has been investigated by comparison of Far-Field patterns, achieved by traditional scanning methods, and by calculation of the Equivalent Noise Level (ENL). The time improvement factor of the new measurement methodology is dependent on the antenna under test and ranges from a minimum of 2.6 to a maximum of 7.5.

***Index Terms*—antenna, satellite, spherical near field, planar near field, measurement.**

I. INTRODUCTION

Standard methods for satellite testing antenna testing are by measurement in a Planar Near-Field (PNF) or Spherical Near-Field (SNF) systems. In such systems, the radiated near field (NF) from the stationary antenna is measured on a planar or spherical surface by a moving probe. The far-field (FF) radiation of the antenna is determined by standard Near-Field to Far-Field (NFFF) transformation [4]. Standard implementations of NF technique are based on dense, regular and equally-spaced NF sampling fulfilling Nyquist criteria. The NF data spacing leads to a much higher number of measurement points than needed and thus longer measurement times.

The method proposed in this paper targets the schedule reduction (and, as a consequence, the associated cost decrease) of satellite antenna testing whilst maintaining the accuracy of standard measurements, using non-canonical and irregular scanning which allows to reduce the number of measurement points. As regards planar measurements, the planar wide-mesh scanning (PWMS) approach [1] has been applied to two telecommunication Ku-band antennas: the numerical model of a shaped reflector antenna, currently flying on a Eutelsat satellite, and the measurements of a pencil beam multi feed reflector antenna. As concerns spherical measurements, a non-canonical scanning [5] has been used for a Galileo navigation antenna [3].

The paper is organized as follows: In Par. II, the non-canonical scanning and irregular sampling approach for planar and spherical NF measurements are briefly presented. Par. III describes the details of the telecommunication and navigation antennas used in the investigation. In Par. IV, the accuracy of the NFFF transform is assessed by comparing traditional acquisition with fast non-canonical sampling transforms with an under-sampling and associated time saving factors ranging from a minimum of 2.6 to a maximum of 7.5. The results are shown in terms of patterns and Equivalent Noise Level. Finally, the conclusions and future activities are summarized in Par. V.

II. NON-CANONICAL SCANNING AND IRREGULAR SAMPLING METHODOLOGIES

To determine the probe voltage V at the points needed to perform the standard NFFF transformations from a nonredundant, i.e. minimum, number of NF samples, it is necessary to remember that, when using a nondirective probe, the voltage V can be well approximated by a bandlimited function [6] having the same effective spatial bandwidth of the antenna under test (AUT) field. According to [6], a quasi-planar AUT can be conveniently considered as enclosed in the smallest two-bowls surface Σ fitting well its shape [1] [5], an optimal parameter ξ must be adopted to describe any curve on the scanning surface and a suitable phase factor $e^{-j\psi}$ must be extracted from the acquired voltage to obtain a spatially quasi-bandlimited function $\tilde{V}$, said "reduced voltage".

A. Planar Wide-Mesh Scanning approach

Unlike the classical plane-rectangular (PR) scanning, the PWMS is characterized by a sample grid with meshes becoming wider and wider with the increase in their distance from the center O' of the scanning plane at $z = d$. This scanning is obtained by adopting the same parameter ξ or η used to represent the x'- or y'- axis for all lines parallel to them. Accordingly, the samples spacing on all lines parallel to the x'- or y'-axis is the same as that for the x'- or y'- axis [1]. Thus, the NF data required by the traditional PR NFFF transformation can be recovered from the PWMS samples by using the following 2-D Optimal Sampling Interpolation (OSI) formula [1]:

$$V(x',y') = e^{-j\psi(x',y')} \sum_{m=m_0-p+1}^{m_0+p} \Big\{ A(\eta(y'),\eta_m,\bar{\eta},N,N'') \cdot \sum_{n=n_0-q+1}^{n_0+q} \tilde{V}(\xi_n,\eta_m) A(\xi(x'),\xi_n,\bar{\xi},N,N'') \Big\} \quad (1)$$

where $n_0 = \lfloor \xi/\Delta\xi \rfloor$, $m_0 = \lfloor \eta/\Delta\eta \rfloor$, $2q \times 2p$ is the number of the retained reduced voltages samples $\tilde{V}(\xi_n,\eta_m)$,

$$\xi_n = n\Delta\xi = 2\pi n/(2N''+1)\,; \quad \eta_m = m\Delta\eta = m\Delta\xi \quad (2)$$

$$N'' = \lfloor \chi N' \rfloor + 1\,; \quad N' = \lfloor \chi' W_\xi \rfloor + 1 \quad (3)$$

$$N = N'' - N'\,; \quad \bar{\xi} = q\Delta\xi\,; \quad \bar{\eta} = p\Delta\eta \quad (4)$$

$\lfloor x \rfloor$ denotes the integer part of x, and χ' and χ are the excess bandwidth and the OSI oversampling factors required to control the bandlimitation and truncation errors [6]. Moreover, the sampling step $\Delta\xi$ is related to the "base bandwidth" W_ξ, which depends on the adopted two-bowls modelling [1], and

$$A(\alpha,\alpha_i,\bar{\alpha},L,L'') = D_{L''}(\alpha-\alpha_i)\,\Omega_L(\alpha-\alpha_i,\bar{\alpha}) \quad (5)$$

is the OSI interpolation function, $D_{L''}(\alpha)$ and $\Omega_L(\alpha,\bar{\alpha})$ being the Dirichlet and Tschebyscheff sampling functions [6].

B. Nonredundant Spherical Scan Approach

According to [5], the following 2-D OSI expansion can be profitably used to recover the NF data needed by the classical spherical NFFF transformation from the nonredundant spherical samples:

$$V(\vartheta,\varphi) = e^{-j\psi(\vartheta)} \sum_{n=n_0-q+1}^{n_0+q} \Big\{ A(\xi(\vartheta),\xi_n,\bar{\xi},N,N'') \cdot \sum_{m=m_0-q+1}^{m_0+q} \tilde{V}(\xi_n,\varphi_{m,n}) A(\varphi,\varphi_{m,n},\bar{\varphi},M_n,M''_n) \Big\} \quad (6)$$

where ξ and φ are the optimal parameters to be used for describing meridians and parallels, respectively [5]. Moreover, $m_0 = \lfloor \varphi/\Delta\varphi_n \rfloor$,

$$\varphi_{m,n} = m\Delta\varphi_n = 2\pi m/(2M''_n+1)\,; \quad M''_n = \mathrm{Int}(\chi M'_n) + 1 \quad (7)$$

$$M'_n = \mathrm{Int}[\chi^* W_\varphi(\xi_n)] + 1\,; \quad M_n = M''_n - M'_n \quad (8)$$

$$\chi^* = 1 + (\chi'-1)[\sin\vartheta(\xi_n)]^{-2/3}\,; \quad \bar{\varphi} = p\Delta\varphi_n \quad (9)$$

the "base bandwidths" W_ξ and W_φ depending on the adopted two-bowls modelling [5] and all the other symbols having the same or analogous meanings as in (1).

III. Test Cases

Three test cases, suitable for planar and spherical NF systems, are presented in this paper:

1) Planar Measurements:
   a) Telecommunication Shaped Beam Antenna;
   b) Telecommunication Pencil Beam Antenna;
2) Spherical measurements:
   c) Galileo Navigation Antenna GIOVE B.

A. Telecommunication Shaped Beam Antenna

The AUT is a large high-performance shaped reflector at Ku-band and is a realistic representation of modern telecommunication antennas with highly shaped coverage embarked on current geostationary satellites such as Eutelsat W [2]. The antenna is a large offset circular reflector with diameter and focal length of 1.8m and feed by a corrugated horn. Preliminary results have been described in [7]. In this study, additional investigations are shown. The optimized antenna is numerically analyzed using standard Physical Optics techniques. This allows to calculate accurately the radiated NF at hypothetical PNF measurement scenarios of any mesh configuration and to calculate accurately the resulting FF for comparison.

B. Telecommunication Pencil Beam Antenna

The pencil beam antenna is a MVG SR40 Reflector antenna (400x315x561 mm) with a feed array of 7 linearly polarized Ku band horns as shown in Fig. 1. For the results shown in this paper, measurements of Beam 5, whose position and U-V maps are shown in Fig. 2, have been employed.

Fig. 1. Pencil beam antenna: SR40 reflector with a feed array

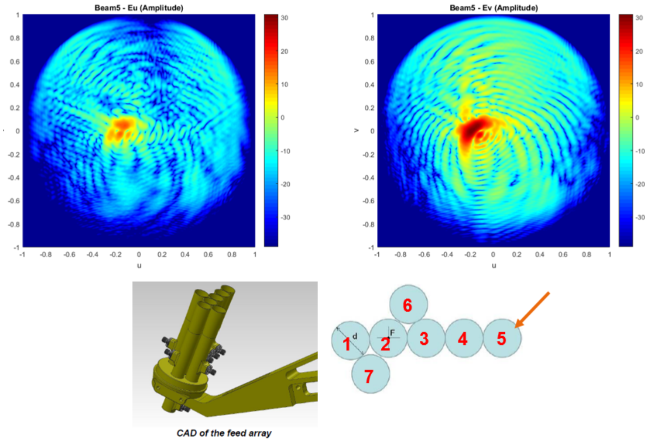

Fig. 2. Pencil beam antenna: Beam 5: postion and UV map

C. *Galileo Navigation Antenna*

The Galileo GIOVE B navigation antenna [3], as shown in Fig. 3, consists of 42 stacked patches on a regular grid within a 1.3 m diameter envelope. The antenna is right hand circularly polarized with an iso-flux pattern, covering an angular domain of +/- 13° (Earth view angle from a Medium Earth Orbit). Measurements performed in ESTEC Hertz scanner [8] by MVG have been used for this paper.

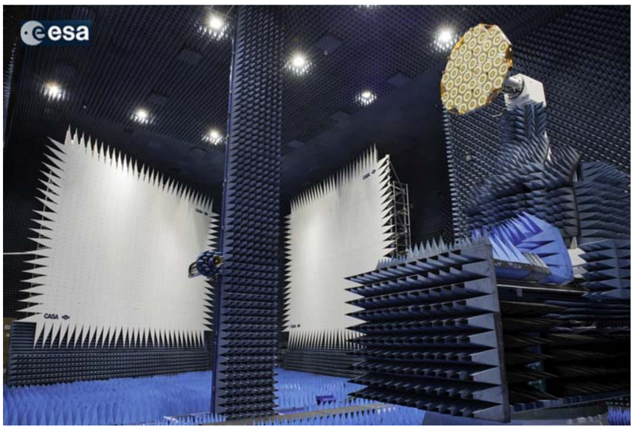

Fig. 3. Galileo GIOVE B Navigation Antenna during measurements in the ESTEC Hertz measurement facility.

IV. COMPARISON OF FAST METHODOLY AND STANDARD APPROACH

For each test case, the comparison is shown in terms of patterns and Equivalent Noise Level [9] comparing the classical and fast non-canonical acquisitions.

A. *Telecommunication Shaped Beam Antenna*

A +/-50° cone centered on boresight allows to reconstruct the main beam and possible disturbing reflections. This results in a scan plane of 8mx8m, with 3m distance from the antenna. With this scan plane, the under-sampling factor by the irregular sampling is 7.5. If a smaller 4x4 m grid is used, as discussed in [7], the under-sampling factor becomes 4.

The FF in terms of copolar and crosspolar components, at phi=0° and phi=90°, is visible in Fig. 4 and Fig. 5 and has been computed from the NF on: classical grid fulfilling Nyquist (PR); PWMS grid; classical grid with decimation, resulting in a sampling step larger than λ/2 (Nyquist criteria).

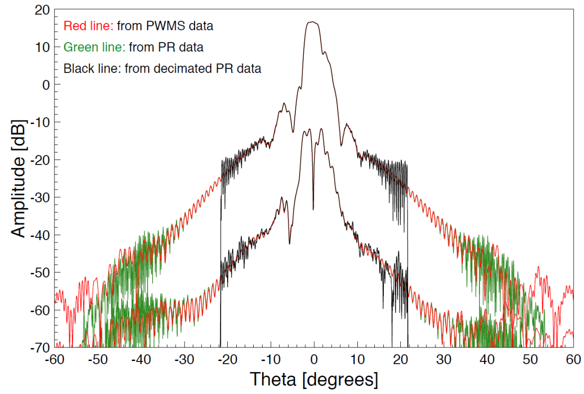

Fig. 4. Shaped Beam Antenna: Copolar and crosspolar components, amplitude, at phi=0°: reconstruction from: PWMS grid (red line), Classical grid with λ/2 sampling step (green line), classical grid with 1.4 λ sampling step (black line).

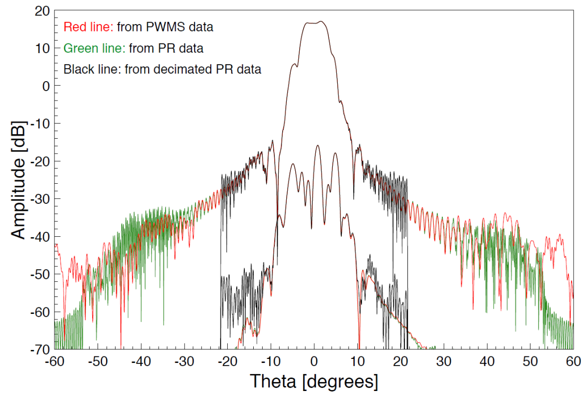

Fig. 5. Shaped Beam Antenna: Copolar and crosspolar components, amplitude, at phi=90°, FF reconstruction from: PWMS grid (red line), classical grid with λ/2 sampling step (green line), classical grid with 1.4 λ sampling step (black line).

The use of decimation is characterized by aliasing affecting the reconstruction angle validity. In fact, the critical angle obtained from the decimated data is +/- 10° which is much smaller than the validity angle achievable with classical acquisition, which is equal to +/- 50°. The decimation could be applied in this case only if: the antenna is very directive; the interest is concentrated on the main beam; both previous information are available a priori. On the contrary, the reconstruction from PWMS data has a more general applicability since it doesn't require a very directive antenna and allows for a very good reconstruction between +/- 50°. In addition to that, due to the filtering properties of the non-redundant interpolation functions, the spatial harmonics relevant to the noise sources outside the AUT spatial bandwidth are cut away.

The Equivalent Noise Level between the reconstruction from PWMS and the PR reconstruction, computed in a theta cone=+/- 25° at phi=0° and phi=90° for the copolar and crosspolar components, 8x8 m scan plane, is shown in Tab.I.

TABLE I. EQUIVALENT NOISE LEVEL FOR TELECOMMUNICATION PENCIL BEAM ANTENNA

Telecommunication Shaped Beam Antenna		
Equivalent Noise Level [dB]		
Phi cut	***CO***	***CX***
Phi=0°	-69.03	-94.31
Phi=90°	-67.45	-99.10

B. *Telecommunication Pencil Beam Antenna*

The non-canonical grid allows an under-sampling factor of 3.8 and requires about 10609 points wrt to 40401 points required by traditional acquisitions. The grids are similar to those shown in [7] for the shaped beam antenna. The comparison for Beam #5, in terms of copolar and crosspolar components, between the FF reconstructed from classical grid fulfilling Nyquist (PR) and PWMS grid, for the cuts phi=0° and phi=90° is shown in Fig.6 and Fig. 7. The difference between the two reconstructions, normalized to the maximum value of the field reconstructed from PR data, is also shown.

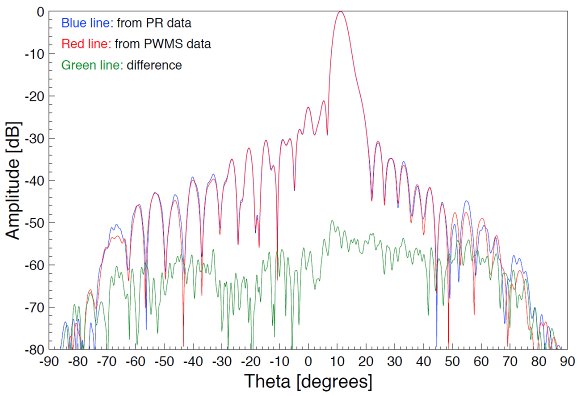

Fig. 6. Pencil beam antenna: Copolar, amplitude, at phi=0°, beam #5, reconstruction from: PR data (classical grid, blue line), PWMS grid (red line) and difference between PR and PWMS grids (green line).

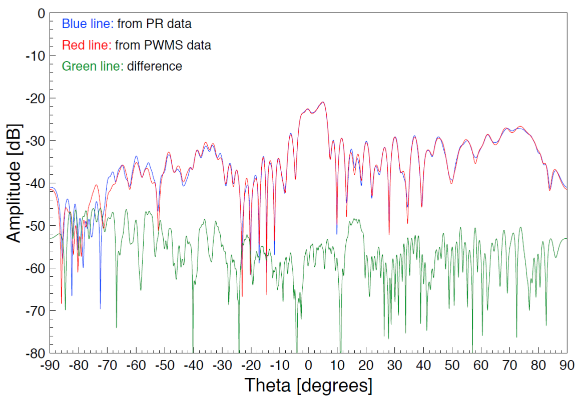

Fig. 7. Pencil beam antenna: Copolar, amplitude, at phi=90°, beam #5 : reconstruction from: PR data (classical grid, blue line), PWMS grid (red line) and difference between PR and PWMS grids (green line).

The Equivalent Noise Level between the reconstruction from PWMS and the PR reconstruction, computed in a theta cone=+/- 25° at phi=0° and phi=90° for the copolar and crosspolar components, beam#5, is shown in Tab.II.

TABLE II. EQUIVALENT NOISE LEVEL FOR TELECOMMUNICATION PENCIL BEAM ANTENNA

Telecommunication Pencil Beam Antenna		
Equivalent Noise Level [dB]		
Phi cut	***CO***	***CX***
Phi=0°	-54.36	-60.65
Phi=90°	-53.96	-57.62

C. *Navigation Giove B Antenna*

The classical spherical grid is composed by 1860 points while the Nonredundant Spherical Scan Approach, both shown in Fig. 8, requires 711 points resulting in an under-sampling factor of 2.6.

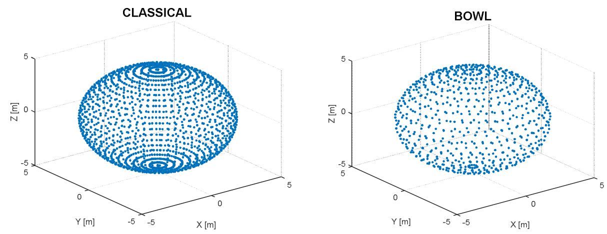

Fig. 8. Galileo Navigation antenna: grids for classical (left) and for Nonredundant Spherical Scan Approach (right) reconstruction.

The comparison, in terms of copolar (RHCP) component, in amplitude and phase, between the FF reconstructed from non-conventional NF spherical grid (blue curve) and the FF reconstructed from classical NF spherical grid (red curve), for the cuts phi=0° and phi=90°, is shown from Fig.9 to Fig. 12. The difference between the two reconstructions, in amplitude, normalized to the maximum value of the field reconstructed from classical NF spherical grid, is also shown.

The Equivalent Noise Level between the reconstruction from non-conventional NF spherical grid and that from classical NF spherical grid, computed in a theta cone=+/- 45°, at phi=0° and phi=90°, for the copolar and crosspolar components, is shown in Tab. III.

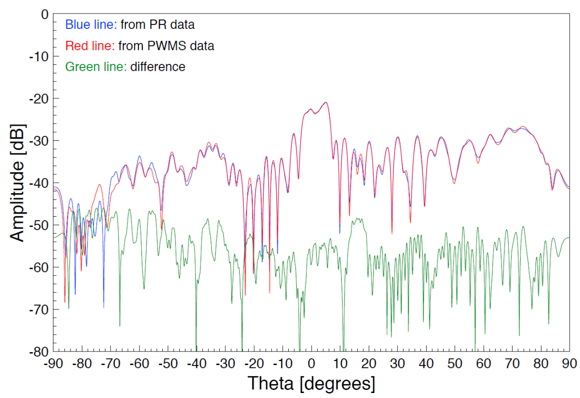

Fig. 9. Galileo Navigation antenna: Copolar RHCP, amplitude, at phi=0° : reconstruction from: non-conventional NF spherical grid (blue line), classical NF spherical grid (red line) and difference between classical and non-conventional grids(green line).

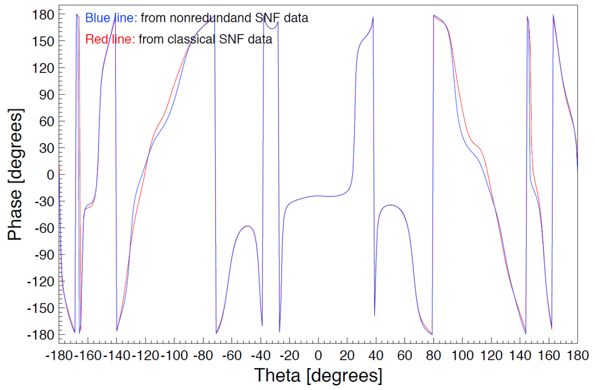

Fig. 10. Galileo Navigation antenna: Copolar RHCP, phase, at phi=0° : reconstruction from: non-conventional NF spherical grid (blue line), classical NF spherical grid (red line).

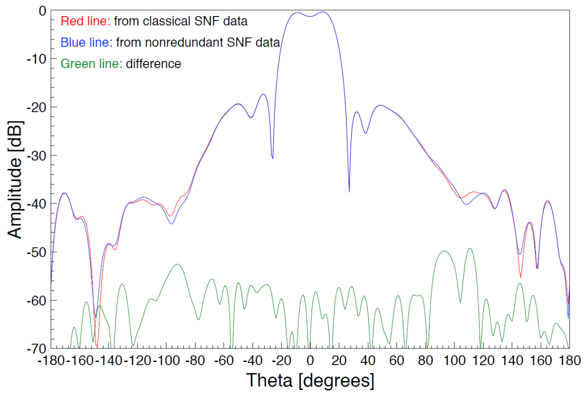

Fig. 11. Galileo Navigation antenna: Copolar RHCP, amplitude, at phi=90°, reconstruction from: non-conventional NF spherical grid (blue line), classical NF spherical grid (red line) and difference between classical and non-conventional grids (green line).

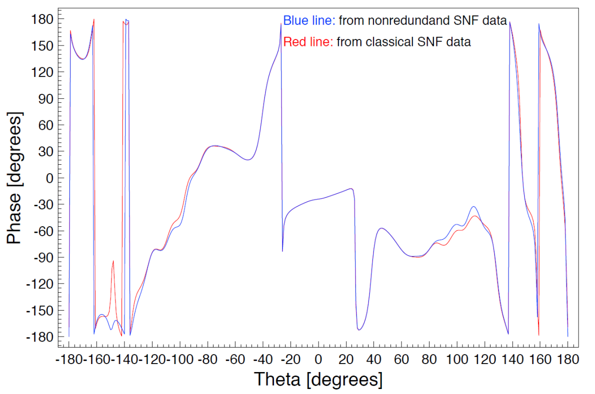

Fig. 12. Galileo Navigation antenna: Copolar RHCP, phase, at phi=90°: reconstruction from: non-conventional NF spherical grid (blue line), classical NF spherical grid (red line).

TABLE III. EQUIVALENT NOISE LEVEL FOR NAVIGATION ANTENNA

Navigation Antenna		
Equivalent Noise Level [dB]		
Phi cut	***CO***	***CX***
Phi=0°	-67.17	-70.34
Phi=90°	-60.20	-66.24

V. CONCLUSIONS

A fast measurement methodology applicable to satellite planar and spherical near field testing using non-canonical scanning and irregular sampling has been presented. Test cases involving Telecommunication and Navigation antennas suitable for planar and spherical test ranges have been analyzed. The achievable under-sampling factor ranges from 2.6 to 7.5. Traditional techniques (fulfilling Nyquist and decimation) have been compared with PWMS and non-redundant spherical scan approach transformations. The very good agreement visible in the presented patterns on the main and side lobes is confirmed by extremely low levels of Equivalent Noise. In particular, the PWMS approach results in a more general applicability than decimation, allowing for a very good reconstruction in the validity angle (defined by classical acquisition). In addition to that, due to the filtering properties of the non-redundant interpolation functions, the spatial harmonics relevant to the noise sources outside the AUT spatial bandwidth are cut away. The actual implementation in standard PNF, such as the ESTEC, Hertz scanner, and SNF ranges is being evaluated and is planned to be experimentally investigated at a later stage.

ACKNOWLEDGMENT

The activities reported in this paper have been partly supported through ESA project “Measurement Methodology For Fast Antenna Testing” (4000121164/17/UK/ND) and through ARTES by the Italian Space Agency.

REFERENCES

[1] F. D’Agostino, I. De Colibus, F. Ferrara, C. Gennarelli, R. Guerriero, M. Migliozzi, “Far-field pattern reconstruction from near-field data collected via a nonconventional plane-rectangular scanning: experimental testing,” Int. Jour. Antennas Prop., vol. 2014, Art. no. 763687, pp. 1-9, 2014.

[2] B Buralli, L. Saussot, E. Schneider, H. Garcia, B. Martel, R. Capone, V. Lubrano, R. Flamini, L. Foged A. Lindley, I. Roberts, “ Dual Gridded Reflecotr Antennas: Final Performance Optimisation Using Prediction and Measurement Technique, AMTA,California, 1999.

[3] https://www.esa.int/Our_Activities/Navigation/Galileo/Satellite_anat

[4] IEEE std 1720 “Recommended Practice for Near-Field Antenna Measurements

[5] F. D’Agostino, F. Ferrara, C. Gennarelli, R. Guerriero, M. Migliozzi, “Effective antenna modellings for NF–FF transformations with spherical scanning using the minimum number of data,” Int. Jour. Antennas Prop., vol. 2011, ID 936781, 11 pages.

[6] O.M. Bucci and C. Gennarelli, “Application of nonredundant sampling representations of electromagnetic fields to NF-FF transformation techniques,” Int. Jour. Antennas Prop. vol. 2012, Art. no. 319856, pp. 1-14, 2012.

[7] M.A.Saporetti, L.J. Foged, M. Sierra Castañer, S. Pivnenko, R. Cornelius, D. Herberling, “Description and Preliminary Results of Antenna Measurement Facility Comparisons in EurAAP”, APM, May 2017.

[8] S. Burgos, P. O. Iversen, T. Andersson, U. Wagner, T. Kozan, A. Jernberg, B. Priemer, M. Boumans, G. Pinchuk, R. Braun, L. Shmidov, “Near-Field Hybrid Test Range from 400 MHz to 50 GHz in the ESTEC Compact Payload Test Range with RF upgrade for high frequencies”, EUCAP 2014."

[9] M.Saporetti, L. Foged, M. Castañer, S. Pivnenko, R. Cornelius, D. Herberling, “Description and Preliminary Results of Antenna Measurement Facility Comparisons in EurAAP”, APM, May 2017.